# Development of a Soft Inflatable Exosuit for Knee Flexion Assistance

Ibrahim Mohammed Hasan, Emiliano Quinones Yumbla, and Wenlong Zhang\*

Abstract—Wearable robotics has shown to be effective for assisting in activities of daily living and restoring motor functions. The objective of this research is to develop a soft robotic exosuit for knee flexion assistance during normal walking and validate its ability to reduce the efforts of the knee flexor muscles: biceps femoris (BF) and semitendinosus (SM). The exosuit is powered by an inflatable curved fabric actuator with the capability to generate flexion torques at the knee joint. An analytical model to characterize the torque of the proposed actuator is derived and validated experimentally. It is found that the analytical torque model precisely matches the experimental results such that the highest root mean square error (RMSE) obtained is 1.237 Nm while the lowest is 0.188 Nm. In addition, the derived model outperformed a benchmark torque model such that its minimum and maximum RMSEs are approximately 90% and 70% less than the benchmark model respectively. A prototype of the knee exosuit is fabricated and tested on one healthy subject with different operating conditions to assist knee flexion during normal walking. The results show that by choosing the appropriate timing of inflation, the exosuit can reduce the electromyography activity of the BF and the SM by 32% and 23%, respectively, without impeding the knee extensor muscle or reducing the knee's range of motion.

#### I. INTRODUCTION

Each year, approximately 795,000 people suffer from stroke in the USA, and many survivors encounter impairment of motor functions post-stroke [1]. For example, reduced knee flexion in the swing phase is a prominent characteristic in stroke patients, which results in reduced step length and walking speed [2]. To fulfill the increased demand for physical therapy, wearable robots have attracted significant attention as potential assistive and rehabilitative devices, and they have shown to be effective in improving motor functions [3] and living independence [4] for impaired users.

Wearable robots can be classified as Exoskeletons and Exosuits. Exoskeletons deliver force/torque to the human's joints using electric motors through rigid links and transmissions [5]. As a result, exoskeletons are often heavy and bulky, resulting in misalignment, discomfort, and even safety risks for the wearer [6]. In contrast, Exosuits are made of lightweight and compliant materials, such as fabrics [7]. In the literature, cable- and pneumatic-driven exosuits have

This material is based upon work supported in part by the National Science Foundation under Grant No. 1944833, in part by Arizona Department of Health Services under Grant ADHS18-198863, and in part by the Global Sport Institute at Arizona State University.

I. Hasan and E. Yumbla are with the School for Engineering of Matter, Transport and Energy, Ira A. Fulton Schools of Engineering, Arizona State University, Tempe, AZ, USA {ihasan2,ejquino1}@asu.edu

W. Zhang is with the School of Manufacturing Systems and Networks, Ira A. Fulton Schools of Engineering, Arizona State University, Mesa, USA wenlong.zhang@asu.edu

been developed for knee rehabilitation and assistance. In [8], the authors developed a cable-driven exosuit for knee extension assistance during stair ascent which reduced the knee's moment and power. In [9] a similar cable-driven exosuit design was developed and showed the potential to reduce the biological power of the knee joint during walking. Also, a wire-driven exosuit was designed in [10] to support the knee joint during stair ascent and descent which showed reduction in muscular activity. Pneumatic-driven exosuits have also shown the potential to assist the knee and reduce muscle activity during activities like normal walking and sitto-stand transfer. A soft exosuit was designed in [11] for knee extension during sit-to-stand employing a pneumatic interference actuator. A novel accordion-inspired actuator for knee extension assistance was introduced in [12] and tested on five human subjects; the electromyography (EMG) results showed a reduction in efforts for the knee extensor muscles. A soft knee exosuit was introduced with inflatable pneumatic actuators made of heat-sealable thermoplastic polyurethane (TPU) for knee extension support [13]. Human testing showed that the exosuit could reduce the knee extensor muscles' EMG activities for healthy participants and improve motor functions for impaired users [14].

Knee flexion is a critical component of human gait as it assists the lower limb to swing and keep the forward progression of the legs [15]. While exoskeletons have studied the effects of assisting knee flexion and showed promising results, providing knee flexion assistance using pneumatic-driven exosuits is still an open problem. Unlike knee extension assistance where an inflatable beam will be sufficient [13], a critical challenge for flexion assistance is finding an appropriate equilibrium flexion angle to match the geometry and curvature of the knee.

In this paper, we present the design, modeling, and preliminary evaluation of a novel soft pneumatic exosuit for knee flexion assistance. The exosuit is powered by a soft inflatable curved flexion actuator specifically designed to fulfill the knee joint's biological, torque and range of motion requirements. In addition, an analytical model of the actuator's torque is developed and experimentally evaluated. Finally, the exosuit prototype is tested on one healthy subject to evaluate the impacts of knee flexion assistance during normal walking.

#### II. KNEE FLEXION EXOSUIT DESIGN

The proposed exosuit should enable: 1) natural torque transmission to the knee with minimal torque loss, 2) simple actuator attachment to prevent slipping during walking, and

<sup>\*</sup>Address all correspondence to this author.



Fig. 1. Overview of the exosuit for knee flexion assistance.

3) adjustable sizes to fit different users. To address these requirements, a soft robotic exosuit was designed, and the prototype shown in Fig. 1 was developed. The exosuit consists of a curved pneumatic-driven interference actuator (CPIA), thigh and shank braces, and an anti-slipping mechanism (including a waist belt and an adjustable buckle connection). We employed inflatable fabric actuators to power the exosuit because they are lightweight, easy to manufacture and have a high power to weight ratio, making them suitable for wearable applications. The actuator is designed for the knee so its distal ends are aligned to the thigh and shank as depicted in Fig. 3. Therefore, if the actuator is inflated at the instant where the knee is about to flex, an assistive torque will arise in the direction of flexion and accordingly assist the knee. The CPIA's physical behavior is similar to a torsional spring but with a stiffness that could be activated (actuator inflated) and deactivated (actuator deflated) as needed.

# A. Knee Biomechanical Torque and Range of Motion

To determine the amount of assistance that the CPIA should provide to the knee, the biological torque and range of motion (RoM) of knee flexion should be determined. The knee flexion starts approximately at 40% of the gait cycle (GC), and it has two peak torques through the GC, one at 40% GC and another at 80% GC [16]-[19]. In this paper, we focus on assisting the knee at the 40% GC peak. The torque values of the first peak in [16]-[19] were averaged, resulting in a peak flexion torque of 14.79 Nm. It's worth mentioning that this peak value corresponds to approximately  $\delta = 0^{\circ}$ . Hence, as the aim here is to partially assist knee flexion, an objective was set to assist with 20% of the peak torque (3 Nm) at 40% GC where  $\delta = 0^{\circ}$ . Moreover, to maintain a natural transmission of the actuator's torque and prevent it from resisting the knee's full extension RoM, the actuator's angle ( $\alpha$  in Fig. 3), needs to be properly designed. According to [16]–[19], the maximum knee flexion angle during normal walking is approximately  $70^{\circ}$ . Therefore, the actuator's angle should be designed to allow a flexion range equal to or bigger than  $70^{\circ}$ . Thus, to give the wearer room for comfort, a design criterion was set that  $\alpha=60^{\circ}$  which allows a flexion range of  $120^{\circ}$ .

#### B. Geometric Features and Manufacturing of the Actuator

The CPIA's geometry is generated by first choosing the actuator's diameter D. Then designing the actuator's angle  $\alpha=60^\circ$ . Afterwards, the inner and outer curvatures are designed to be tangents to the straight ends of the actuator. To avoid stress concentration, the radii of the circular arcs are needed to be considerably large. For this purpose, we have manufactured different actuators with different curvatures' radii. Afterwards, each actuator has been placed on the platform Fig. 4 at a flexion angle  $\delta=0^\circ$ , and then inflated to the maximum pressure used in experiments which is 35 psi. As a rule of thumb from this experiment, setting the radius of the inner arc to be  $\geq D$  and the radius of the outer arc to be  $\geq 2D$ , will avoid stress concentration and failure at the curved regions within the 35 psi pressure range.

As shown in Fig. 1, the proposed actuator consists of an inflatable plastic tube made of a TPU (American Polyfilm Inc., Branford, CT) and an outer nylon fabric shield (Seattle Fabrics. Inc., Seattle, WA). The TPU layers are cut using a stencil and heat-sealed together with an heat sealer from all sides except one end. Similarly, the two fabric layers are sewed together by a sewing machine while leaving the end unstitched. Then, the TPU tube is inserted inside the fabric shield and a pipe fitting gland is pinched through the TPU and fabric layer and threaded by a mechanical nut to prevent air leaks. Finally, the open end of the TPU tube is heat-sealed and the fabric layer is stitched.

## C. Braces' Design and Manufacturing

The braces' function is to transfer the actuator torque to the knee, clamp the actuator to the leg, and enable adjustable sizes. As demonstrated in Fig. 1, the thigh and shank braces are designed to be modular and curved parts that are connected by hinges. The braces are attached to the thigh and shank by using fabric straps with Velcro attached to their ends. This structure gives the wearer the flexibility to tighten and loosen the braces as much as needed. Also, the integration of the Velcro with the hinged modular parts allows size adjustability such that it can fit different wearers. In addition, the braces are 3D printed using polylactic acid (PLA), which are advantageous over fabric braces in resisting torsion and thus reduces transmission losses. Finally, to prevent slipping of the exosuit during walking, the thigh brace is anchored to the hip by a waist belt. The complete wearable exosuit design weighs approximately 700 g, making it a lightweight device.

# III. ANALYTICAL TORQUE MODEL OF THE ACTUATOR

This section discusses the derivation of an analytical torque model based on the principle of virtual work. The

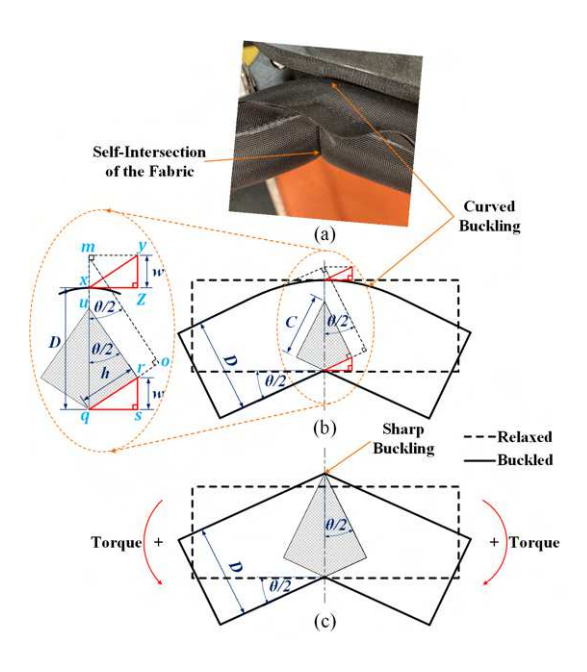


Fig. 2. (a) Experimental observation of the buckled actuator. Folded Volume approximation of: (b) Model I, and (c) Model II [20].

inflated pneumatic fabric actuator produces a resistive torque when it is loaded by an external torque that makes it buckle. This resistive torque reacts to the change in the internal volume and fluidic pressure inside the actuator. The actuator's volume decreases because the actuator physically folds to accommodate the external load as shown in Fig. 2(a). Simultaneously, the internal pressure increases because the volume decreases. To model this behavior, the principle of virtual work is applied as follows

$$\tau = P \frac{dV(\theta)}{d\theta},\tag{1}$$

where  $\tau$  is the torque produced by the actuator,  $\theta$  is the buckling angle, P is the pressure in the actuator and  $V(\theta)$ is the actuator volume as a function of  $\theta$ . From (1), there should be an analytical formula for  $V(\theta)$  in order to estimate the torque at any given  $\theta$  and P. In [20], the authors proposed an analytical model for  $V(\theta)$  of a similar Pneumatic Interference Actuator (PIA), where they assumed that the actuator buckles to have a sharp profile and the folded volume was modeled to be the hatched region in Fig. 2(c). However, our experimental observation shows that the actuator buckles forming a curved profile as indicated in Figs. 2(a)-(b). This curved profile forms because the actuator is physically constrained to keep its diameter constant. This means that the formed curve is circular and has a radius that is equal to the actuator's diameter,  $D = \overline{xq}$ , and a center that coincides with the self-intersection point, q in Fig. 2(b). Based on this observation, we hypothesize that folded volume is the hatched region illustrated in Fig. 2(b).

To obtain a closed-form analytical model for  $V(\theta)$ , the trigonometry Fig. 2(b) is studied. From point x, the vertex of the curvature, we draw  $\overline{xy}$  which is parallel and equal to  $\overline{qr}$ . Then we form the right triangles  $\Delta xyz$  and  $\Delta qrs$  which are identical as they have equal hypotenuses as well as equal

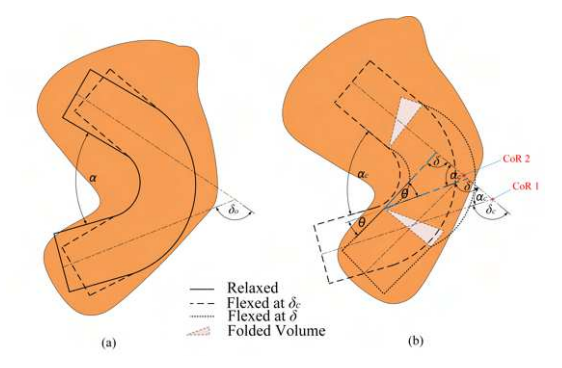


Fig. 3. (a) Knee and CPIA configuration before buckling. (b) Knee and CPIA configuration after buckling.

legs. Then we find  $w=\overline{mq}-\overline{xq}$ , where  $\overline{mq}=D\sec\left(\frac{\theta}{2}\right)$  from  $\Delta qom$ , and  $\overline{xq}=D$ . Looking at triangle  $\Delta qrs$ , we find  $h=w\csc\left(\frac{\theta}{2}\right)$ . Thus,  $C=h\cot\left(\frac{\theta}{2}\right)$  from triangle  $\Delta qru$ . Therefore, the folded volume can be calculated as follows,

$$V(\theta) = \frac{\pi}{4} D^2 L - \frac{\pi}{4} C^2 h$$
 (2)

where, L is the actuator's original length which is constant. By finding the derivative of the actuator's volume described by (2) with respect to the buckling angle and substituting into (1), the actuator's torque formula results as below,

$$\tau = -\pi D^3 P \frac{3\cos\left(\frac{\theta}{2}\right) - 3\cos^2\left(\frac{\theta}{2}\right) + 1}{8\cos^2\left(\frac{\theta}{2}\right)\left(\cos\left(\frac{\theta}{2}\right) + 1\right)^3}.$$
 (3)

As shown in Fig. 3, the CPIA buckles and forms two folded volumes. These folds are identical to the folds that result from buckling two straight actuators, PIAs, with the same diameter by the same angle  $\theta$ . Nevertheless, the torque produced by the CPIA equals the torque produced only by one straight PIA. That is because two folded volumes form such that they are mechanically connected in series in that curved configuration. This is similar to the same physical behavior of the actuator developed in [11].

To solve (3) for torque and validate it experimentally,  $\theta$ , P, and D should be determined. Theoretically, the actuator generates torque if it's slightly flexed from  $\delta_o$ , defined in Fig. 3(a), to any other flexion angle  $\delta$ . In this case,  $\theta$  is defined as  $\theta = \delta_o - \delta$ , where  $\delta_o = 180^\circ - \alpha$ , and  $\alpha$  is the actuator's design angle in the relaxed state as shown in Fig. 3(a). Practically, the actuator has some extensibility as the fabric material is not completely inextensible. In addition, the interaction between the fabric shield and the internal TPU tube could possibly allow slippage between the fabric layer and the TPU layer. Therefore, the actuator does not buckle at  $\delta_c$ , rather, it extends until it reaches a critical flexion angle  $\delta_c$ as demonstrated in Figs. 3(a)-(b). At this angle of  $\delta_c$ , if the actuator is further flexed to another angle  $\delta$ , it buckles and generates torque. Therefore the buckling angle is now defined as  $\theta = \delta_c - \delta$ . This angle  $\delta_c$  could be modeled analytically using a similar approach as in [21]. Nevertheless, to simplify the procedures,  $\delta_c$  will be determined experimentally as explained in the next section.

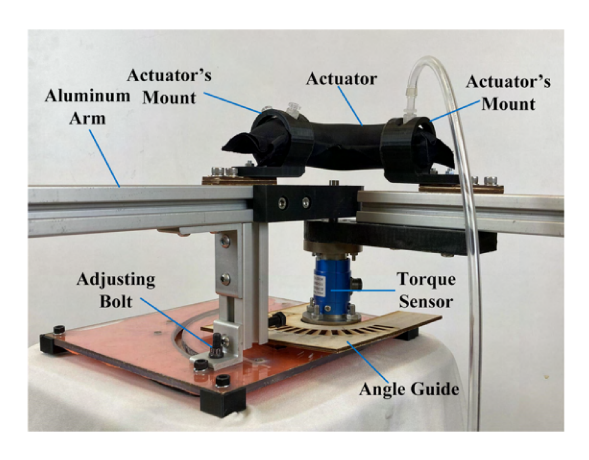


Fig. 4. Experimental setup for torque characterization of the soft actuator.

#### IV. ACTUATOR CHARACTERIZATION

#### A. Test Setup and Experimental Procedures

To calculate  $\delta_c$  and validate the analytical model, an experimental setup was built as shown in Fig. 4. The experimental setup consists of a torque sensor (Forsentek Co, China) and two aluminum arms connected by a revolute joint to mimic the knee joint. Five actuators with different diameters were tested on the platform in Fig. 4 at  $\delta = 0^{\circ}$  and different pressure values. All five actuators were fabricated with  $\alpha = 60^{\circ}$  and inner and outer curvatures' radii of D and 2D respectively. The experiment showed that an actuator with D=4 cm achieves the 3 Nm torque requirement at an applied pressure P = 20 psi. Therefore, this actuator was chosen as the candidate actuator for experimental testing and validation. To determine  $\delta_c$  of the candidate actuator, it was mounted on the testing platform at its relaxed state  $(\delta = 120^{\circ})$ , and the flexion angle was decreased gradually from 120° until a state where a slight further decrease in the flexion angle forms folds and generates a positive torque on the readings of the torque sensor. This experiment was repeated three times which eventually showed that the critical flexion angle of the candidate actuator is approximately  $\delta_c = 90^{\circ}$ .

Afterwards, the candidate actuator was experimentally tested to validate the pressure-torque relationship at different pressures and flexion angles. In the experiment, at a given flexion angle, the torque values were recorded as the pressure changed from 0 to 35 psi in increments of 5 psi. Each experiment was repeated three times and the results were averaged. This procedure was performed in a flexion angle range from  $0^{\circ}$  to  $90^{\circ}$  in increments of  $10^{\circ}$ . The pressure-torque results at all given flexion angles are demonstrated in Fig. 5.

#### B. Torque Characterization Results and Discussion

The experimental results are compared with the proposed analytical model in (3), denoted as analytical Model I, and the model in [20], denoted as analytical Model II. Results in Fig. 5 demonstrate that Model I is clearly outperforming Model II in all testing conditions, specially at high flexion angles,  $\delta = 50^{\circ}$ ,  $70^{\circ}$ ,  $80^{\circ}$ , and  $90^{\circ}$  where it had RMSEs of

0.567, 0.623, 0.188, and 0.626 Nm, respectively On the other hand, Model II shows significantly larger RMSE values than Model I at all testing conditions and the highest RMSE is 4.09 Nm at  $\delta=0^\circ$  while the lowest is 2.39 Nm at  $\delta=60^\circ$ . Overall, these findings support the hypothesis of the folded volume approximation shown Fig. 3(b) which experimentally validates the improved accuracy of our model compared to the benchmark. Finally, it is observed that, at 90° flexion angle, the actuator experimentally has negative torque values at high pressures, shown in Fig. 5(j). This negative torque is because the actuator forms opposite folds in the inner curved region as a result of a misalignment between the actuator and the aluminum arms center of rotation.

#### V. HUMAN TESTING

# A. Testing Protocol

The human subject testing consisted of three conditions: baseline (exosuit was not worn), inactive (exosuit was worn but never inflated), and active (exosuit was worn and periodically inflated during walking). For all conditions, the subject walked for 5 minutes at their preferred speed. The active session consists of 4 sessions that correspond to 4 different delay values to trigger the inflation, as discussed in Sec. V-B. All the testing sessions were randomized. After each session, the subject was asked to rest for at least 10 minutes to avoid muscle fatigue. Before starting experiments, maximum voluntary contraction (MVC) trials were conducted for the EMG data normalization. The experimental protocol was approved by the Arizona State University Institutional Review Board (STUDY00011110).

During the experiment, the subject walked on an instrumented split-belt treadmill (Bertec Inc., Columbus, OH) equipped with two force plates to measure the ground reaction forces sampled at 1,000 Hz. Sixteen reflective markers were placed on the subject's lower body to capture motion data at 100 Hz using the optical motion capture system (T40s, VICON Inc., Los Angeles, CA). Smart shoe sensors [22] that measure ground reactions forces were used to detect gait events for control of the exosuit. To measure the muscle's activity, EMG sensors (Delsys Trigno, Delsys, Natick, MA) with a sampling frequency of 2,000 Hz were placed on the knee flexor (BF and SM) and extensor (vastus lateralis) muscles. One healthy subject of 75 kg and 1.70 m was recruited with a 0.7 m/s preferred walking speed and a required knee flexion torque of 3 Nm.

#### B. Control Strategy

The goal of the exosuit is to provide knee flexion assistance during the swing phase. The ideal timing to assist knee flexion is at 40% GC as identified in [16]–[19], but the delays in the actuator response require starting the inflation earlier. This study intends to validate that, while delays are present in the actuator response, the exosuit can successfully assist human gait. Moreover, we seek to understand the effects of inflation timing on the human muscular responses in order to maximize the benefits of the exosuit in future works. In this paper, the inflation time was explored by choosing

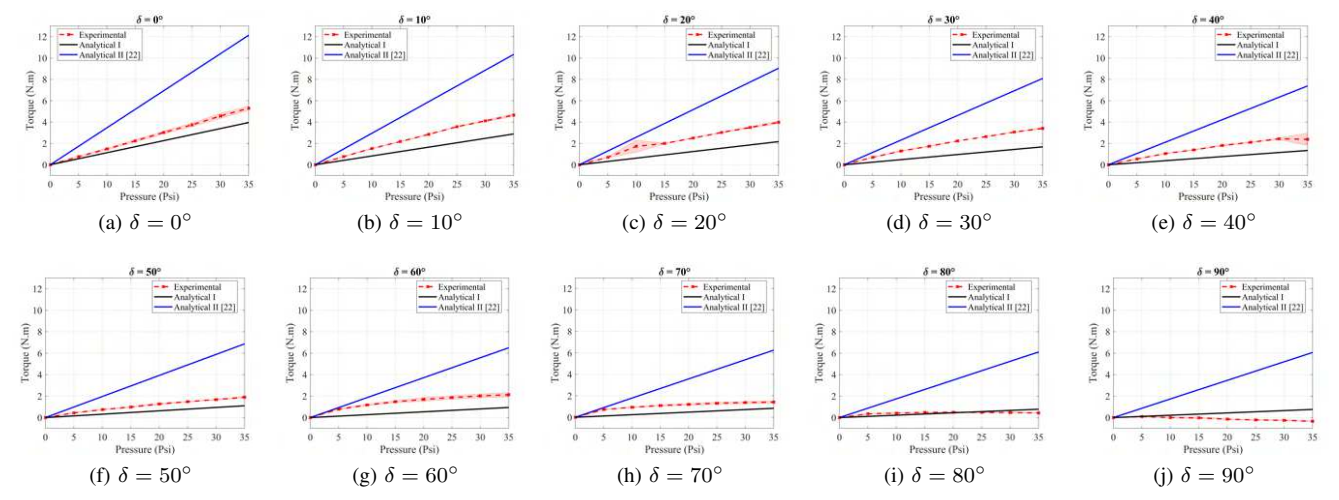


Fig. 5. Comparisons between the proposed torque model and a benchmark model against experimental results at different flexion angles

different offset values, after detecting heel strike, which corresponds to 35%, 32% and 25% of the GC. The offset values were selected to allow building internal pressure so that by 40% GC the actuator is stiff and provides sufficient flexion torque. With the torque model it was identified that an internal pressure of 20 psi satisfies the 3 Nm torque required to assist the subject. As a preliminary study, a bang-bang controller was implemented to inflate the actuator to 20 psi at the desired offset time after heel strike and then deflate at the maximum knee flexion angle. The heel strike event is detected by the smart shoe. The maximum knee flexion event is found by averaging the time interval from heel strike to maximum knee flexion of all gait cycles of the baseline session.

## C. Results and Discussion

The EMG data were filtered by a 4th-order bandpass Butterworth filter. Kinematic and EMG data were segmented into gait cycles and temporally normalized to percent GC. The average and standard deviation for each data point across different gait cycles was computed to obtain a representative plot of the joint kinematics and EMG activity.

Table I summarizes the average change in the EMG of the muscles investigated, namely BF, SM, and the Vastus Lateralis (VL) over all gait cycles compared with the baseline session. The results show that the exosuit can reduce the average EMG activity of the flexor muscles (BF and SM) with all the offset values for inflation. It's observed that, 35% GC inflation time showed the most reduction of knee flexor muscle activities EMG, with a maximum reduction of 26% and 35.6% for the BF and SM with compared to baseline, respectively. One explanation for this result is that early inflation of the exosuit triggers an earlier and higher activation magnitude of the flexion muscles during the terminal stance phase from approximately 30% to 50% GC as observed in Fig. 6a and Fig. 6b. Furthermore, early inflation of the exosuit can induce resistance to the extensor muscles and an increase in the VL EMG activity, as observed from 50% to 60% GC in Fig. 6c and Table I. In addition,

TABLE I
COMPARISON OF EXPERIMENTAL RESULTS IN DIFFERENT CONDITIONS

Inflation (% GC)	BF (%)	SM (%)	VL (%)	RoM
25	-19.7	-20.4 *	9	37.5°
32	- 23	- 32 *	- 2.85	$56.2^{\circ}$
35	- 26 *	- 35.56 *	0.27 *	$37.4^{\circ}$
Inactive	- 0.1	- 3.7	5.2	$37.5^{\circ}$
Baseline	-	-	-	$57.46^{\circ}$

<sup>\*</sup> indicates statistical significance (p < 0.05)

examining the results for the inactive condition in Table I shows that wearing the exosuit does not significantly alter the EMG activity of the muscles, which implies that the exosuit does not induce significant resistance to the wearer and it is a transparent device for daily use.

The average knee joint kinematics profile of the complete walking trial for two offset values (25% and 32% GC) are presented in Fig. 7, and the corresponding range of motion (RoM) is summarized in Table I. The baseline and inactive cases show a similar pattern, especially during the stance phase. However, the knee RoM was significantly reduced when the exosuit was worn, except for the 32% GC case. A possible reason for the reduced RoM is that the user might become conservative when he experienced the tightened velcro of the exosuit, or some resistance when the exosuit was inflated too early or late. In summary, inflating the exosuit at 32% GC leads to a similar knee RoM and significantly reduced knee flexor muscle activities, without impeding the knee extensor, compared to the baseline. It is thus the most appropriate time to inflate the exosuit for this user. The preliminary results with the exosuit provide early evidence of its efficacy in assisting knee flexion motion, and highlight the importance of designing personalized control strategies for different users.

# VI. CONCLUSIONS

In this paper, we presented the development and preliminary evaluation of a soft pneumatic exosuit to assist knee flexion. A curved pneumatic interference actuator was

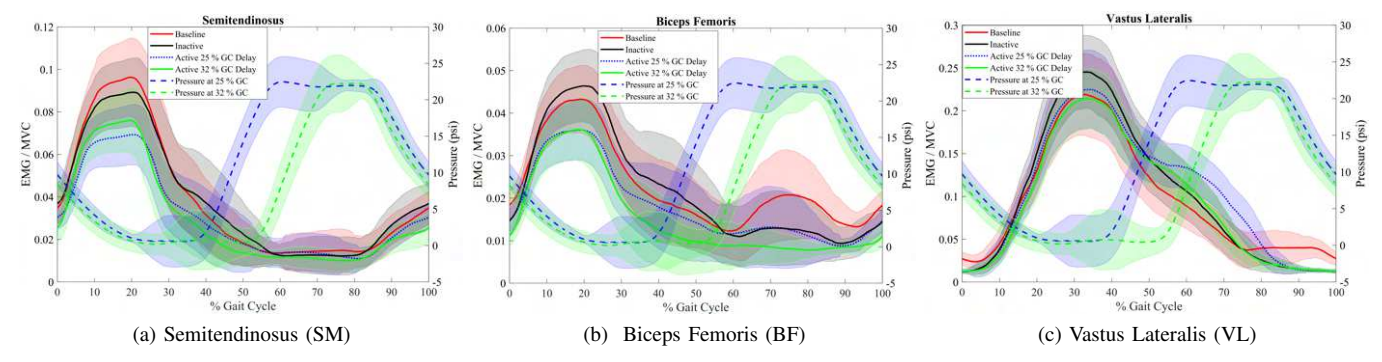


Fig. 6. EMG results of different muscles for the 32% and 25% GC inflation time.

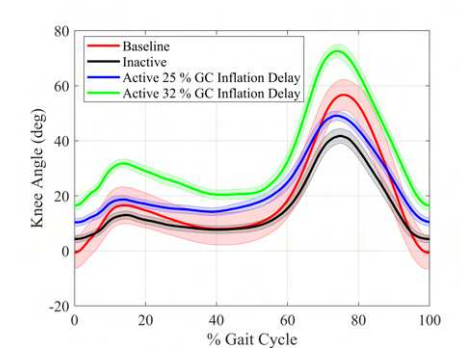


Fig. 7. Knee joint kinematics for different inflation times.

designed to generate flexion torque at the knee joint. An analytical torque model to characterize the actuator's torque was derived. The model was evaluated experimentally, and it outperformed a benchmark model at all testing conditions. The exosuit was tested on one healthy subject while walking at a self-selected speed. EMG measurements showed that the exosuit reduced activities of knee flexor muscles in all testing conditions, and the percentage of reduction varied with the time of inflation. The preliminary results showed the efficacy of the exosuit in assisting knee flexion during normal walking and provides initial results to understand the effects of inflation timing of pneumatic exosuits.

Future work remains on developing an analytical model of the actuator that describes the critical flexion angle  $\delta_c$ . In addition, we will develop an intelligent controller to select the ideal inflation time and pressure inside the actuator. The flexion actuators will be combined with the extension actuators [13] into a single design to assist the knee motion in the complete gait cycle. Finally, we will test with more subjects to show its impact on daily assistance and gait rehabilitation.

#### REFERENCES

- [1] S. S. Virani *et al.*, "heart disease and stroke statistics 2020 update: A report from the american heart association."
- [2] E. Hutin et al., "Lower limb coordination patterns in hemiparetic gait: Factors of knee flexion impairment," Clin. Biomech., vol. 26, no. 3, pp. 304–311, 2011.
- [3] S. E. Fasoli, B. Ladenheim, J. Mast, and H. I. Krebs, "New Horizons for Robot-Assisted Therapy in Pediatrics," Am. J. Phys. Med. Rehabil., vol. 91, no. 11, pp. S280–S289, nov 2012.
- [4] C.-A. Smarr et al., "Older adults' preferences for and acceptance of robot assistance for everyday living tasks," Proc. Hum. Factors Ergon. Soc. Annu. Meet., vol. 56, no. 1, pp. 153–157, 2012.

- [5] A. M. Dollar and H. Herr, "Lower extremity exoskeletons and active orthoses: challenges and state-of-the-art," *IEEE Trans. Robot.*, vol. 24, no. 1, pp. 144–158, 2008.
- [6] D. Zanotto, Y. Akiyama, P. Stegall, and S. K. Agrawal, "Knee Joint Misalignment in Exoskeletons for the Lower Extremities: Effects on User's Gait," *IEEE Trans. Robot.*, vol. 31, no. 4, pp. 978–987, aug 2015
- [7] E. Q. Yumbla, Z. Qiao, W. Tao, and W. Zhang, "Human assistance and augmentation with wearable soft robotics: a literature review and perspectives," *Curr. Robot. Rep.*, vol. 2, pp. 399–413, 12 2021.
- [8] G. Huang et al., "A biologically-inspired soft exosuit for knee extension assistance during stair ascent," in 2020 5th IEEE Int. Conf. Adv. Robot. Mechatron. (ICARM), 2020, pp. 570–575.
- [9] H. D. Lee, H. Park, B. Seongho, and T. H. Kang, "Development of a Soft Exosuit System for Walking Assistance During Stair Ascent and Descent," *Int. J. Control. Autom. Syst.*, vol. 18, no. 10, pp. 2678–2686, oct 2020.
- [10] E. J. Park et al., "A Hinge-Free, Non-Restrictive, Lightweight Tethered Exosuit for Knee Extension Assistance During Walking," *IEEE Trans. Med. Robot. Bionics*, vol. 2, no. 2, pp. 165–175, may 2020.
- [11] A. J. Veale, K. Staman, and H. van der Kooij, "Soft, Wearable, and Pleated Pneumatic Interference Actuator Provides Knee Extension Torque for Sit-to-Stand," *Soft Robot.*, vol. 8, no. 1, pp. 28–43, feb 2021.
- [12] J. Fang et al., "Novel Accordion-Inspired Foldable Pneumatic Actuators for Knee Assistive Devices," Soft Robot., vol. 7, no. 1, pp. 95–108, feb 2020.
- [13] S. Sridar, Z. Qiao, N. Muthukrishnan, W. Zhang, and P. Polygerinos, "A soft-inflatable exosuit for knee rehabilitation: Assisting swing phase during walking," *Front. Robot. AI*, vol. 5, p. 44, 2018.
- [14] S. Sridar *et al.*, "Evaluating immediate benefits of assisting knee extension with a soft inflatable exosuit," *IEEE Trans. Med. Robot. Bionics*, vol. 2, no. 2, pp. 216–225, 2020.
- [15] L. Zhang et al., "Knee Joint Biomechanics in Physiological Conditions and How Pathologies Can Affect It: A Systematic Review," Appl. Bionics Biomech., vol. 2020, pp. 1–22, apr 2020.
- [16] S. H. Collins, M. B. Wiggin, and G. S. Sawicki, "Reducing the energy cost of human walking using an unpowered exoskeleton," *Nature*, vol. 522, no. 7555, pp. 212–215, jun 2015.
- [17] K. Shamaei et al., "Design and evaluation of a quasi-passive knee exoskeleton for investigation of motor adaptation in lower extremity joints," *IEEE Trans. Biomed. Eng.*, vol. 61, no. 6, pp. 1809–1821, jun 2014.
- [18] Y. Ding et al., "Biomechanical and physiological evaluation of multijoint assistance with soft exosuits," *IEEE Trans. Neural Syst. Rehabil*itation Eng., 2017.
- [19] W. van Dijk and H. Van der Kooij, "Xped2: A passive exoskeleton with artificial tendons," *IEEE Robot. Autom. Mag.*, vol. 21, no. 4, pp. 56–61, 2014.
- [20] C. R. Nesler, T. A. Swift, and E. J. Rouse, "Initial Design and Experimental Evaluation of a Pneumatic Interference Actuator," *Soft Robot.*, vol. 5, no. 2, pp. 138–148, apr 2018.
- [21] C. T. O'Neill et al., "Unfolding Textile-Based Pneumatic Actuators for Wearable Applications," Soft Robot., jan 2021.
- [22] P. T. Chinimilli, S. W. Wachtel, P. Polygerinos, and W. Zhang, "Hysteresis Compensation for Ground Contact Force Measurement With Shoe-Embedded Air Pressure Sensors," in *Proc. ASME* 2016 Dyn. Syst. Control Conf., vol. 1, oct 2016.